Tire wear mechanisms and how they relate to wear particle sizes – a brief review

Alexander Schmiedhofer, Pierluigi Bilotto and Carsten Gachot
Institute for Engineering Design and Product Development, Research Unit Tribology, TU Wien, Vienna, Austria

Abstract

Purpose – The new EURO 7 regulation will set limits on non-exhaust emissions, which include tire wear. Therefore, this study aims to develop a comprehensive understanding of how tire wear particles are formed, their size distribution, and the influence of factors such as vehicle weight, speed, and road surface conditions.

Design/methodology/approach – Tire wear is caused by three different mechanisms: Cut and chip (abrasion), fatigue, and chemical wear. Each mechanism appears differently, thus each of them is described separately in a respective chapter.

Findings – All three wear mechanisms can occur at all times, but, depending on the tearing energy, one is usually dominant: Cut and chip happen at high energy levels, fatigue at medium energy levels, and chemical wear at low energy levels. Each mechanism produces different particle sizes, from the mm to the nm range, but most commonly in the range of 2.5 μm–10 μm.

Originality/value – A lot of research has been done on tire and rubber wear, but the size of wear debris particles was often an afterthought, therefore, this work summarizes all available information on this topic.

Peer review – The peer review history for this article is available at: https://publons.com/publon/10.1108/ILT-08-2025-0372/

Keywords Tire, Rubber, Wear, Abrasion, Particle size, Cut and chip, Fatigue, Smearing, Pavement, Abrasion pattern

Paper type Literature review

1. Introduction

Since the beginning of the 21st century, the pollution caused by microplastics (polymer particles between 1 μm and 5 mm) and its impact on the environment has become a major focus of scientific research (Browne *et al.*, 2007). Among the various sources of microplastics, tire wear has emerged as one of the most significant contributors. Comprehensive studies conducted in Germany (Essel *et al.*, 2015), Denmark (Lassen *et al.*, 2015), and Norway (Sundt *et al.*, 2014) have all identified dust from vehicle tires as the largest single source of microplastic emissions. In 2015 alone, approximately 6.4 million tonnes of synthetic rubber were produced globally for tire manufacturing (Boucher and Friot, 2017), and it is estimated that nearly one billion tires reach the end of their service life each year (Yadav and Tiwari, 2017). In the European Union, 3.2 million tonnes of used tires were generated in 2013 (CINARALP, 2015). Tire wear has been estimated to contribute approximately 5% to 10% of the total global microplastics entering the oceans (Kole *et al.*, 2017), highlighting the urgent need for a better understanding and mitigation of microplastic pollution from this source. This is especially worrying as most particles end up in rivers, lakes or oceans, and have a profound negative impact on aquatic species (McCarty *et al.*, 2023; Wagner *et al.*, 2014; Chae and An, 2017).

Interest in tire wear as a source of particulate matter has intensified following the proposal of the EURO7 regulation (European Commission, 2024), which aims to establish limits on non-exhaust emissions (particles generated from vehicle tires and braking systems). The implementation of diesel particulate filters has already led to a reduction of over 99% in exhaust emissions of diesel vehicles within the PM_{10} and $PM_{2.5}$ size fractions (Bergmann *et al.*, 2009), resulting in minimal differences in exhaust emissions among electric, gasoline, and diesel-powered vehicles. Consequently, non-exhaust particles now account for more than 90% of total PM emissions, with approximately 10% attributed specifically to tire wear (Timmers and Achten, 2016).

This review aims to provide a comprehensive introduction to particulate matter, with a specific focus on particles generated through tire wear. We begin by discussing the fundamental

The current issue and full text archive of this journal is available on Emerald Insight at: **https://www.emerald.com/insight/0036-8792.htm**

Industrial Lubrication and Tribology
78/2 (2026) 231–242
Emerald Publishing Limited [ISSN 0036-8792]
[DOI 10.1108/ILT-08-2025-0372]

The authors acknowledge funding via the research project *Green Tire* (grant #5121078) from the Austrian Ministry of Finance and administered by the Austrian Research Promotion Agency (FFG). The authors further acknowledge TU Wien Bibliothek for financial support through its Open Access Funding program.

Conflict of interest: The authors declare no conflict of interest.

Received 14 August 2025
Revised 7 October 2025
Accepted 11 November 2025

characteristics of particles and proceed to examine the tribological mechanisms underlying tire wear. Experimental approaches and simulation methods commonly used to study these processes are also reviewed.

While existing literature on tire wear is extensive, most studies either focus on lab experiments to determine wear rates of rubber (Muhr and Roberts, 1992; Saibel and Tsai, 1969; Schallamach, 1954; Fukahori *et al.*, 2020) or on collecting particles from roadways and analyzing their composition and size distribution (Zhang *et al.*, 2023; Grigoratos and Martini, 2014). An additional challenge arises from the lack of standardization in this field. Tire abrasion can be examined from tribological, materials science or vehicle dynamics perspectives, each employing distinct analytical methods with different focal points. Even within a single discipline, variations in experimental design, parameter selection, and particle collection protocols hinder the comparability of results across studies. Therefore, a central objective of this work is to consolidate and critically assess the available data specifically related to theoretical and empirical predictions of tire wear particle sizes. Finally, we offer perspectives on emerging research directions and potential advancements in this field.

Tire wear particles form in the contact zone between the tire tread and the road surface. In general, tires consist of multiple materials that each perform a different function. The main materials constituting tires are listed, with sources, in Table 1.

From this variety of materials, natural rubber (NR) and synthetic rubber are prominent. The former gives the tire tread elasticity and flexibility and has good tensile strength, tear resistance and chemical resistance properties. The latter, e.g. styrene-butadiene rubber (SBR), improves hardness and has higher abrasion resistance than NR. Their combination forms a compound that provides the best properties of both materials.

Fillers are used as reinforcements to improve hardness, wear, and UV resistance, and softeners to improve the stickiness and wet grip performance. Steel and textile fibers increase stiffness, vulcanization agents accelerate the vulcanization process, and additives help to protect the tire against degradation by ozone, oxygen and heat (Piscitello *et al.*, 2021).

In addition to their chemical composition, the size of tire particles plays a crucial role in their environmental and health impacts. Real-world data indicate that a significant amount of emitted particles fall within the size range of 2.5 μm to 10 μm (Lassen *et al.*, 2015, p. 124). Particles in this range are linked to an increased risk of cardiovascular and cerebrovascular diseases, as they can trigger systemic inflammation, promote blood clotting, and even enter the bloodstream (Anderson *et al.*, 2012). As a result, many field studies focus on measuring particles within this size range (Gustafsson *et al.*, 2009; Aatmeeyata *et al.*, 2009; Hussein *et al.*, 2008; Kupiainen *et al.*, 2005; Sjödin *et al.*, 2010; Panko *et al.*, 2009). However, some of these studies were not equipped to capture larger particles. Notably, other experiments using different methodologies have detected tire particles with size distributions centered around 20 μm to 80 μm (Kreider *et al.*, 2010; Xu *et al.*, 2025).

Tire wear is closely linked to the texture and quality of the road surface. Concrete and asphalt are the most commonly used pavement types. A typical concrete mixture consists of approximately 6% air, 11% Portland cement, 41% aggregate (crushed stone or gravel), 26% sand, and 16% water. In contrast, asphalt is composed of 95% aggregates bound together by bitumen (Ivel *et al.*, 2020).

An exemplary particle size distribution is shown in Figure 1, where particles were collected on a plate, mounted on the frame of a car, immediately downstream of a tire (Dannis, 1974). The size and number of emitted particles were measured on a road with a concrete surface at velocities of 72 km/h and 105 km/h, and on an asphalt surface at 105 km/h. The results showed that driving on concrete produces more particles than on asphalt. The particle size appears to be log-normal distributed, where increasing velocity decreases the mean value, and the asphalt surface increases the standard deviation compared to the concrete pavement.

The impact of the road surface on tire wear was also investigated in (Allen *et al.*, 2006), where tire wear was measured indirectly using chemical markers. The study was conducted in a tunnel that was initially paved with Portland Cement Concrete (PCC) and later resurfaced with Asphalt Rubber - Asphaltic Concrete Friction Course (AR-ACFC). Marker compounds present in tire tread material, exhaust gases, and aerosol samples were collected at the tunnel's entrance and exit. Comparisons revealed that tire emission rates were 1.4–2 times higher on the PCC surface than on the AR-ACFC pavement.

The differences between porous (double-layered porous asphalt concrete, DLPAC) and dense (stone mastic asphalt, SMA) pavements were examined in (Lundberg *et al.*, 2020). Porous pavement can reduce traffic noise and lower PM_{10} emissions by trapping dust particles, however, it is less durable and therefore rarely used in Nordic countries, where studded tires are common. The study analyzed mineral dust loads (particles < 180 μm) and found that emissions peaked during winter months, decreasing by a factor of 4–5 in the summer for both pavement types. While the total particle emissions across the wheel tracks (left, right, and center) were similar for both DLPAC and SMA, the dense SMA pavement showed PM concentrations 8–10 times higher at the road edges. The particle size distribution is centered around 20 μm, with the DLPAC distribution slightly shifted toward larger sizes.

Table 1 Typical composition of a car tire (Wik and Dave, 2009) [1], (Piscitello *et al.*, 2021) [2], (Wagner *et al.*, 2018) [3], (Sommer *et al.*, 2018) [4]

Category	Ingredients	Content in Wt.%	Source
Rubber/Elastomer	Natural rubber (NR), Styrene butadiene Rubber (SBR), Butadiene rubber (BR)	40–60; 40–50	[1],[2],[3];[4]
Reinforcing agent (filler)	Carbon black (CB), silica	20–35; 30–35	[1],[2],[3];[4]
Process oils, Extender oils softener	Mineral oils, resin	15–20; 12–15; 15	[1];[2],[3];[4]
Textile & Metal net	Kevlar, nylon, steel	5–10; 5–12	[2];[3]
Vulcanization agent	S, ZnO	4; 1–2; 2–5	[1];[2],[3];[4]
Additives	Preservatives Anti-oxidants plasticizers	1; 5–10	[1];[2],[3],[4]

Figure 1 Particle size distribution on concrete and asphalt at different speeds, data taken from Dannis (1974)

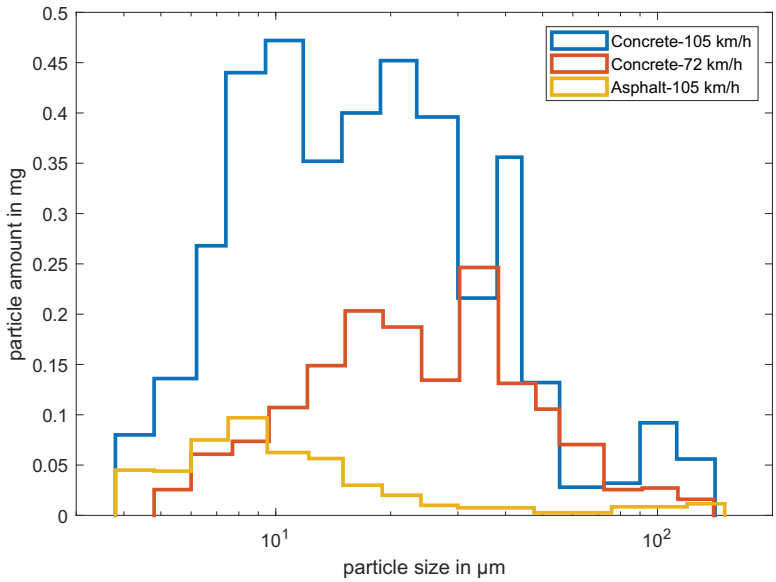

Gustafsson *et al.* (2009) focused on the impact of aggregate material and size in asphalt concrete, combined with different tire types (studded, winter and summer). The results showed that granite pavements produced approximately 70% more PM_{10} than quartzite pavements of the same aggregate size. Between two quartzite pavements with different aggregate sizes, the one with a maximum size of 16 mm generated roughly three times more emissions than the one with a maximum size of 11 mm. In addition, studded tires produced about ten times more PM_{10} emissions than standard winter tires, while summer tires contributed a negligible amount.

Another important factor in tire wear is vehicle weight, as tire abrasion is caused by friction between the tire and the road, which increases with the normal force exerted by the vehicle. Furthermore, resuspension of road particles is influenced by the size and aerodynamic properties of a vehicle, with larger vehicles generally generating more resuspension due to their greater mass (Timmers and Achten, 2016). Consequently, tire wear is generally assumed to be positively correlated with vehicle weight, a hypothesis that has been investigated and partially confirmed in several studies (Simons, 2016; Garg *et al.*, 2000). This is especially relevant because the mass and front area of new car models have increased by 66% and 22% respectively, between 1980 and 2018 (Weiss *et al.*, 2020). In addition, the weight of electric vehicles is on average 20% higher than their ICE counterparts (Mueller *et al.*, 2024) and by 2050, 35% to 60% of all cars sold in the US could be electric (medium outlooks (Muratori *et al.*, 2021).

While numerous factors influencing the size of tire debris particles have been discussed, the particle size is ultimately governed by the underlying wear mechanisms. In the existing literature, tire wear is typically categorized into three main mechanisms: cut and chip (CC) abrasion, fatigue or pattern wear, and chemical or smearing wear.

CC wear occurs when individual surface asperities or irregularities remove fragments of the tire tread, resulting in scratches aligned with the direction of sliding. Fatigue or pattern wear arises from repeated loading cycles on relatively smooth surfaces, leading to crack formation, culminating in wear patterns oriented perpendicular to the sliding direction. Chemical or smearing wear is driven by local heat buildup, shear stress, and environmental factors such as oxygen, ozone, and UV radiation, which chemically degrade the rubber compound.

Each mechanism is associated with a characteristic particle size range. Chemical wear can produce an oily residue (Gent and Pulford, 1983), while volatilization processes generate nanoparticles (Park *et al.*, 2017). In contrast, CC wear typically results in larger particles, which may agglomerate with pavement debris to form conglomerates ranging from 220 μm to 1230 μm in size (Adachi and Tainosho, 2004). This finding was confirmed by an investigation in which particles were collected using an instrumented vehicle equipped with an on-board system capable of determining the mass-weighted size distribution (Truong *et al.*, 2025). In that study, the authors attributed elongated and rough-textured particles to fatigue wear, with average particle sizes ranging from approximately 12 μm in suburban environments to more than 50 μm on rural roads. In addition, they identified smoother, rounder, and more irregular particles, which they suggested originated from local vaporization and subsequent condensation of tire compounds. These particles exhibited average sizes between 0.6 μm on highways and 2 μm on urban roads. In the following chapters, a detailed examination of each wear mechanism is provided.

2. Cut and chip wear

If tires are subjected to harsh conditions (e.g., riding on a gravel road), they experience a wear phenomenon often termed CC wear (Stoček *et al.*, 2021a). Cutting takes place when the tire hits a sharp object with enough force to penetrate the surface. Chipping then occurs because traction, breakage, or other forces cause the initiation of a tear in the rubber compound,

Industrial Lubrication and Tribology
Volume 78 · Number 2 · 2026 · 231–242

usually at a 90° angle to the direction of the cut, removing a piece of tire thread (Beatty and Miksch, 1982).

Experimentally, CC can be investigated with an *Instrumented Chip and Cut Analyzer (ICCA)*, where a rotating rubber sample is impacted by a stainless-steel tool with a specified frequency. After some revolutions, cracks with distinct angles form on the surface of the material, which grow in length and number, eventually intersecting, which leads to small chips of rubber being removed. The cracks in SBR appeared to grow deeper than in NR, creating larger wear particles. In contrast, the impact process progressed much more rapidly for the BR compound, leading to a higher abrasion rate and early material failure (Stoček *et al.*, 2019).

The influence of the material on CC damage was further investigated with an ICCA using an impactor of 2.5 mm radius (Stoček *et al.*, 2021b). At a lower normal force ≤ 130 N, a 40 NR/60 SBR blend was more resistant, and at a higher force > 130 N, pure NR developed less damage. This is due to the higher intrinsic strength of SBR compared to NR, but at higher load, strain-induced crystallization occurs in NR, increasing its strength (Treloar, 1975).

For another material, hydrogenated nitrile rubber (HNBR), a linear relation was found between frictional work and the average particle diameter. This was tested by pressing a quartz sample (Mohs hardness 5.5–6.5) on a rotating rubber disk (modified Du Pont Abrader) (Thavamani and Bhowmick, 1992).

Numerical methods to describe abrasion at the asperity level are discussed in (Zhang *et al.*, 2022), which gives some insight into the two classic theories of the Archard wear law and Rabinowicz criterion, the Finite Element Method (FEM) with realistic elastic-plastic material behavior, and molecular dynamics (MD) simulations.

In (Wu and Shi, 2013) FEM was used to confirm a previous theory (Suh, 1973) on how wear particles form in the contact of two metal asperities: First, the fracture initiates and propagates in the trailing portion of the contact area, followed by a second smaller fracture that emerges at the leading contact edge. Finally, the two fractures propagate and link below the contact area, forming a flake-like wear particle.

The contact of two asperities was also simulated using MD (Brink and Molinari, 2019). It was assumed that each asperity is hemispherical with diameter d and that when they touch, the formed junction interface is inclined by the angle θ relative to the direction of movement. It was found that exists a critical d^* and θ^* for a certain strength of the adhesive interface that determine whether the said asperities slide past each other, plastically deform or adhere to each other and form a wear particle. The critical length scale d^* was also investigated in (Aghababaei *et al.*, 2016), in which the authors found a function for d^* that accurately predicts if a debris particle is formed from the asperities or if they are plastically deformed and smoothed.

It should be noted, however, that all simulations were done with no specific material in mind (or with materials that behave like metals), and therefore, no effects unique to rubber were considered. Expanding and completing the simulation framework, including rubber-like materials, is an important research direction for the next decades.

In the end, the mechanism of wear is influenced by many factors, a fact nicely demonstrated by multiple experiments. When (Muhr and Roberts, 1992) abraded unfilled NR on silicon carbide paper in the presence of a lubricant, score lines in the direction of motion formed on the rubber surface, indicating CC wear. If no lubricant is applied, even though the CoF increased only slightly (1.34 vs 1.23), the score marks are replaced by a wear pattern. Similarly, an experiment on the aforementioned Du Pont abrader showed that NR and SBR formed a wear pattern, while in HNBR, fine scratch marks in the direction of abrasion are observed (again indicating CC wear). However, when the same experiment was repeated at 50°C, HNBR a wear pattern appeared as well (Thavamani and Bhowmick, 1993). The formation of a wear pattern perpendicular to the sliding direction indicates that a different wear mechanism is dominant: Fatigue.

3. Fatigue wear

It is well-known that rubber on a smooth surface does not slide continuously but in a stick-slip motion. This is caused by rubber molecules adhering to the surface, getting stretched along the direction of movement (stick phase), detaching and relaxing (slip phase), before they start to adhere to the surface again (Schallamach, 1963; Persson and Volokitin, 2006).

This was further explored by sliding a steel slider, of the razor blade type, over a block made from natural rubber, in reciprocal motion, while measuring the frictional force and the acceleration (Fukahori and Yamazaki, 1994b). Results show a stick-slip motion with a frequency f_{ss} of 10 Hz to 20 Hz (decreasing with increasing normal force), where the frictional force increases during the stick phase and decreases in the slip phase in a periodic, sine-like manner. The acceleration is negligible in the stick phase, but shows violent micro-vibrations of a higher frequency (500 Hz–1000 Hz) during the slip phase. A further analysis revealed that this frequency of the micro-vibrations matches the intrinsic natural frequency of the rubber f_0, which was measured separately.

During micro-vibrations on the rubber surface, upward motion causes it to adhere to the slider. The resulting high relative sliding velocity generates frictional forces that induce a significant stress concentration at the edge of the small contact area, leading to the formation of the first micro-crack in the rubber. When the rubber surface detaches and subsequently readheres to the slider, a second micro-crack forms at a distance:

$$d_0 = \frac{v}{f_0} \tag{1}$$

from the first, where $v.$ is the sliding velocity and f_0 is the natural frequency of the used rubber sample. This theoretical value was compared to the optically measured distance between the micro-cracks on the rubber sample. This relationship was confirmed for NR with multiple different velocities (Fukahori and Yamazaki, 1994b). The pattern spacing d_0 then increases with the number of slidings, very similar to how small streams converge into a main river, until a critical value $d_0 = D_0$ is reached, after which the pattern spacing stays constant and can be estimated similarly to equation (1):

$$D_0 = \frac{v}{f_{ss}} \tag{2}$$

using the stick-slip frequency f_{ss} instead of the natural frequency. The formation of micro-cracks is sketched in Figure 2(a).

Even after a stable wear pattern has formed on the rubber surface (an exemplary wear pattern is shown in Figure 3), micro-cracks are continually formed on top of larger ridges, which creates wear particles in a size range from tens of micrometers or less up to hundreds of micrometers (Cadle and Wiliiams, 1978; Dannis, 1974).

The presented theory of pattern formation was also confirmed to apply to filled NR and SBR. Reinforcement by carbon black increases the stiffness of the material and therefore increases the initial and stick-slip frequency, which gives a smaller initial and final pattern spacing. Furthermore, the additional damping decreases the propagation speed of the surface waves, thus increasing the necessary number of cycles until a steady-state wear pattern is formed. Both effects lead to a smaller abrasive wear in more filled rubbers (Fukahori and Yamazaki, 1994a).

The underlying mechanism of fatigue wear is crack growth within the material. This is schematically shown in Figure 2(b). As the blade passes over the pattern, the tongue of rubber is pulled back and then released as the blade moves on. The stress produced by this process is assumed to cause crack growth (Southern and Thomas, 1978). Initially, the crack propagates at a low slope relative to the surface, until a critical length is reached, after which it turns upwards to form a new wear particle. When looking at fatigue crack growth from a fracture mechanics standpoint, it is therefore important to consider crack growth perpendicular to the surface. Experimental data suggest that, if the rate of growth is the same, then the whole time it takes to create the wear particle is more than twice the propagating time of the low slope (Uchiyama and Ishino, 1992; Southern and Thomas, 1978).

Notably, stick-slip motion is not a unique phenomenon to rubber friction but can occur in any sliding contact if the difference between the static and dynamic coefficients of friction is large enough. If the material is considered as a damped harmonic oscillator, the transition from a stick to a slip phase acts as a displacement. Therefore, subsequent vibration in the (damped) natural frequency is very much expected (Bowden and Tabor, 2001; Gao Chao *et al.*, 1994). This could also explain the influence of the normal force on the stick-slip frequency, because the load directly influences the friction coefficient of rubber (Fortunato *et al.*, 2017).

The linear rate of abrasive wear $\dot{D}$ can be estimated from the crack growth rate dc/dn if the mean strain ε^* in the stress field, produced by frictional sliding, is accurately evaluated, see equation (3) (Fukahori and Yamazaki, 1995).

$$\dot{D} = \frac{dc(\varepsilon^*)}{dn} \tag{3}$$

Once the wear pattern stabilizes in size, and assuming perfect stick during the stick phase, the mean strain amplitude can be expressed as follows:

$$\varepsilon^*_{\mathrm{id}} = \frac{L_{st}}{L_{sl}} = \frac{\mu P}{ES} \tag{4}$$

where L_{st} and L_{sl} are the distances the slider moves in the stick and slip phase, respectively, μ is the friction coefficient, P is the normal load, E is the Young's modulus of the rubber, and S is the deformed cross-sectional area, approximated by $S = hd$, with h being the width of the rubber specimen and d the indentation depth of the slider. The unique combination of properties of rubber materials, high friction, low modulus, and high deformability, is the reason why periodic surface patterns form on rubber but rarely on other materials. In reality, however, perfect slick does not take place even in the stick phase (also micro-vibrations are still generated), and the slider moves a certain distance Δr in the stick phase. The formula for the mean strain can be adapted to accommodate this:

$$\varepsilon^*_{\mathrm{ac}} = \frac{L_{st} - \Delta r}{L_{sl}} \tag{5}$$

The actual and ideal mean strain values calculated match perfectly with the authors' experiments (Fukahori and Yamazaki, 1995). The results also show that the rate of crack growth is not improved by the use of carbon black as a filler agent, at low strain rates, it is even faster than in unfilled

Figure 2 This diagram shows a circular slider moving over a rubber surface with velocity *v*. (a): At first, micro-cracks are initialized, (b) After enough revolutions, a steady state wear pattern forms, and wear particles form via crack propagation

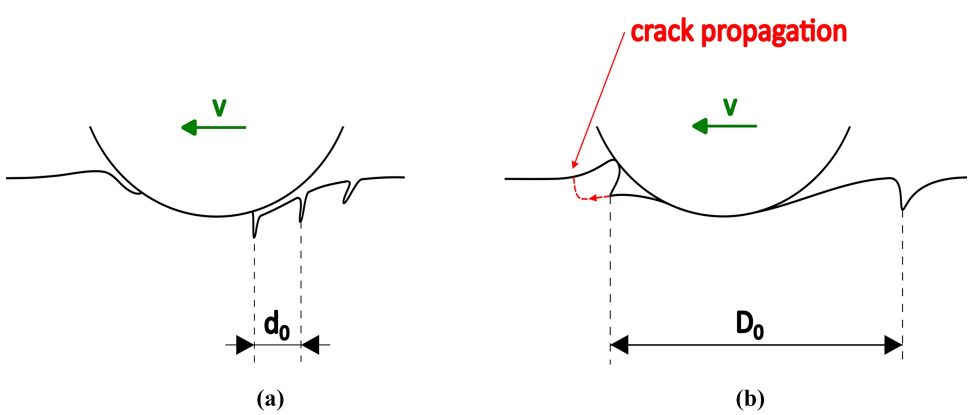

Figure 3 Wear patterns formed by a blade indenter pressing on a rotating rubber disk after 2000 cycles (Reproduced under the term of the CC-BY Creative Commons Attribution 4.0 International license (https://creativecommons.org/licenses/by/4.0/) (Setiyana *et al*., 2021). Copyright 2021, Setiyana *et al*., MDPI)

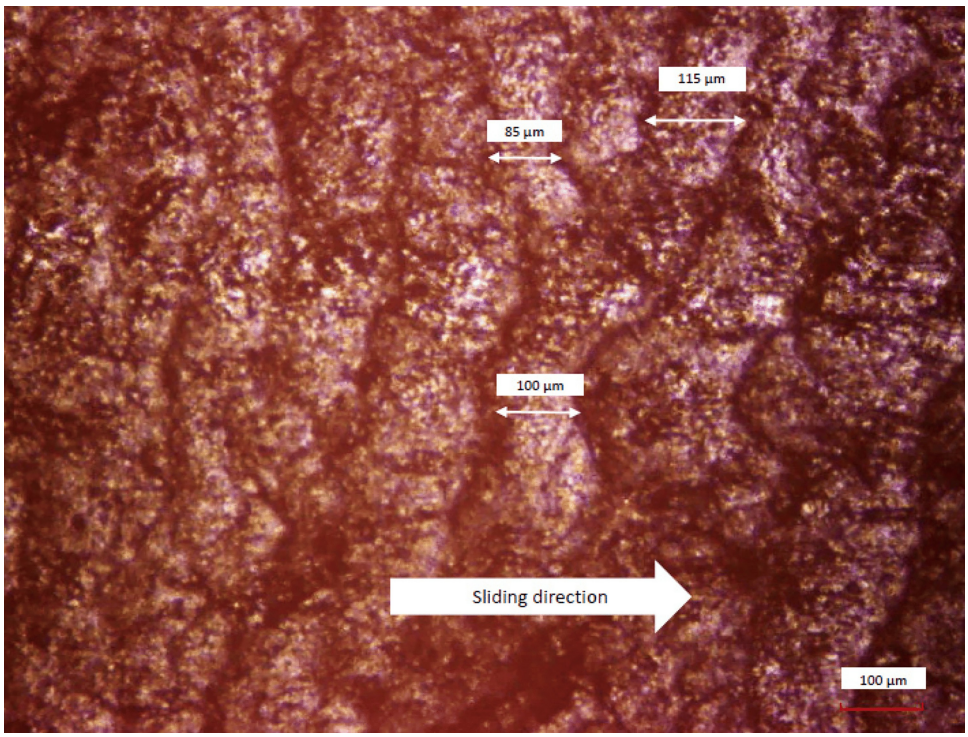

rubbers. However, as the carbon black content increases, E increases, μ increases slightly, and S decreases, which according to equation (4) drastically decreases the strain ε^* and therefore the wear rate per equation (3).

Earlier experiments on pattern wear of rubber with sandpaper have already shown some proportional relations [equation (6)] between the pattern spacing D_0, the normal load per unit area L, the curvature of the abrasive particle r, the diameter of the abrasive particle d, and the Young's modulus E (Schallamach, 1954):

$$D_0 \propto \left(\frac{Lrd^2}{E}\right)^{1/3} \tag{6}$$

If the abrasive can be approximated to a set of close-packed hemispheres (as a simplified model of an asphalt surface), the following relation can be made:

$$\frac{\dot{D}}{D_0} = \left(\frac{L}{E}\right)^{2/3} \tag{7}$$

This linear increase in additional wear due to pattern formation with pattern spacing was also observed in other experimental data (Schallamach, 1968a, 1968b). Other results (Southern and Thomas, 1978) found that pattern spacing is directly proportional to the frictional force (per unit width).

The equations presented in this chapter should be applied with caution, as rubber wear is a highly complex phenomenon influenced by numerous parameters, as previously discussed at the end of Chapter II. For instance, different rubbers can exhibit varying wear pattern spacings even when subjected to similar modulus and load conditions (Southern and Thomas, 1978). There is evidence suggesting that the proximity to the glass transition temperature (T_g) plays a significant role. In the case of NBR ($T_g = -30°C$), the wear pattern is not pronounced at 20°C, but becomes more distinct as the temperature increases. Conversely, rubbers such as NR and SBR, with lower glass transition temperatures ($T_g = -55°C$ and $-70°C$, respectively), exhibit a much coarser pattern at 20°C, which tends to become finer with increasing temperature.

The coefficient of friction and the presence of lubrication also significantly affect abrasion behavior, as described by Eq.4. In one study (Setiyana *et al.*, 2021), tests conducted under identical parameters, but one dry and one with a thin layer of low-viscosity oil, showed no meaningful difference in pattern spacing, consistent with the observation that the measured friction coefficients were nearly identical. However, other results (Muhr and Roberts, 1992) demonstrated that the wear pattern can completely disappear when a lubricant is applied, due to the reduced frictional forces. Additional experiments (Muhr *et al.*, 1987) indicated that friction force may not be the dominant factor, as the wear rate was found to decrease by several orders of magnitude, which is far more than the reduction in the friction coefficient alone would suggest. Furthermore, evidence of strongly nonlinear behavior has been reported (Evstratov, 1967), with the wear rate dropping sharply when the friction coefficient falls below a critical threshold.

The formation of a wear pattern is prevented if the direction of the abrader is reversed after every run. Wear under these conditions is called *intrinsic abrasion*, and it is closely connected to the tensile strength of the rubber material. The abrasion rate and the size of abraded particles, created under these circumstances, are significantly lower (Schallamach, 1954; Schallamach, 1958; V H Nguyen *et al.*, 2017).

Directional effects were investigated using the Grosch wheel experiment, in which a small rubber wheel is pressed against a rotating abrasive disk (V H Nguyen *et al.*, 2017). By adjusting the wheel's orientation, different slip angles relative to the rolling direction were imposed. The slip angle was periodically varied under three conditions: (a) +45° to −45°, (b) +45° to +60°, and (c) held at constant 0°. The results revealed that the wear rate was the highest for the largest slip angle variation, following the trend: (a) > (b) > (c). Remarkably, the accumulated material damage exhibited the opposite trend, with the 0° slip condition, which corresponds to pattern wear, causing the greatest damage. Over time, however, differences in both wear rate and damage diminished, converging toward similar steady-state values across all slip angle conditions.

When NR is abraded against a smooth surface, such as finely ground glass, the temperature rise due to frictional heating, ΔT, has been shown to scale with the sliding velocity v, normal force F, and a material-dependent exponent α (Schallamach, 1957):

$$\Delta T \propto \sqrt{v} F^{\alpha} \tag{8}$$

This frictional heating softens the rubber and increases the real contact area, generally leading to a decrease in the CoF with increasing normal load (Schallamach, 1955; Fortunato *et al.*, 2017). The CoF also exhibits a nonmonotonic dependence on sliding velocity, showing a Gaussian-like peak centered around v ≈ 1 mm/s, spanning several orders of magnitude. This behavior is observed on both smooth and rough (e.g., asphalt) surfaces. Temperature rise under frictional loading has also been studied using a thermocouple sliding against a rotating rubber disk (Schallamach, 1958). Results show that temperature increases more rapidly at lower normal loads, attributed to reduced heat conduction due to less flattening of surface asperities. Consequently, softer materials tend to exhibit lower surface temperatures during friction, despite lower thermal conductivity.

It may be surprising that fatigue, a phenomenon associated with blunt tracks, can be investigated by scraping with a razor blade. However, the sharpness of the blade has no influence on the wear pattern formation, as long as it is sufficiently sharp so that only one element of the wear pattern is deformed at a time (Southern and Thomas, 1978). Furthermore, lubricants drastically decrease the rate of blade wear, as explained earlier, even if the mechanism is not fully understood. These two findings indicate that, especially for a dry contact, frictional stress, rather than cutting, is primarily responsible for the wear (Muhr and Roberts, 1992). Also, while many experiments about pattern wear are carried out on a blade abrader, wear patterns are observed in real tire-road contact (Schallamach, 1958; Grosch and Schallamach, 1961).

If the normal force, and consequently the frictional energy, are sufficiently low, a sticky layer can develop on the rubber surface instead of a typical fatigue wear pattern. This phenomenon is known as chemical wear (M Huang *et al.*, 2018).

4. Chemical wear

Under relatively mild wear conditions, certain rubber materials (CB-filled compounds of SBR, NR, and EPR) exhibit the formation of an oily, sticky and degraded surface layer, a phenomenon known as smearing wear (Wu *et al.*, 2023). This wear debris is characterized by a higher concentration of volatile components [11.12% vs 8.13% in NR, and 10.23% vs 8.75% in SBR filled with 50 phr CB (parts per hundred rubber)] as well as elevated oxygen content (41.7% vs 39% in NR and 8.5% vs 2.8% in SBR with CB). Although T_g remains similar, the molecular weight is about an order of magnitude lower than that of the bulk material, accounting for its sticky, liquid-like morphology.

A significant de-crosslinking effect has also been observed (Wu *et al.*, 2023), with reductions of approximately 75% in NR and 55% in CB-filled SBR. This suggests thermo-mechanical degradation of the three-dimensional rubber network. Evidence of devulcanization is further supported by solubility tests in toluene: Freshly generated smearing wear debris is completely soluble, while samples exposed to air for over 24 h become insoluble. A likely mechanism involves the formation of free radicals under loading conditions – arising from the scission of polymer backbones or crosslinks, followed by radical scavenging facilitated by filler particles and antioxidants.

This behavior has been corroborated by previous studies (M Huang *et al.*, 2018), which additionally report that aged smearing wear debris can be redissolved following brief sonication. This suggests the formation of bound rubber, where the polymer interacts with filler particles through relatively weak physical or chemical associations.

This microstructural phase separation within a polymer is illustrated in a series of SEM images in Figure 4 (Koliolios *et al.*, 2024). The leftmost image provides an overview of the fractured wear surface, revealing a flake-like texture indicative of layered material failure. A zoomed-in section in the middle panel offers a closer view of the microstructure, highlighting heterogeneous regions within the material. Further magnification on the right distinguishes two distinct phases: The upper inset shows a dark, textured region where carbon black particles are densely clustered and closely interact with the polymer matrix, resulting in a more rigid, constrained phase. In contrast, the lower inset reveals smoother, layered structures representing polymer areas with little to no filler interaction. This clear phase separation supports the conclusion that smear wear layers exhibit weaker mechanical properties due to the loss of uniform filler dispersion and the emergence of mechanically distinct polymer domains.

The formation mechanism of smearing wear was long not fully understood (Gent and Pulford, 1983), however, oxygen appears to play a significant role in the process. This was confirmed by conducting an abrasion experiment with the same material under the same conditions, only once in an oxidative environment, and once in an oxygen-free atmosphere (Nakano *et al.*, 2021). In the absence of oxygen, the rubber produced a powdery substance, while in the presence of oxygen, smearing wear occurred.

This oxygen-dependent behavior was also observed in a similar experiment (Gent and Pulford, 1979), and the abrasion rate increased eightfold under oxidative conditions. Comparable wear rates were recorded in inert environments such as nitrogen, argon, or vacuum, indicating that the absence of reactive species prevents smearing. Interestingly, when a free-radical-trapping compound, such as thiophenol, was

Figure 4 SEM images show the phase separation of the rubber polymer and carbon black (Adapted under the terms of the CC-BY Creative Commons Attribution 4.0 International license (https://creativecommons.org/licenses/by/4.0/) (Koliolios *et al*., 2024). Copyright 2024, Koliolios *et al*., Elsevier)

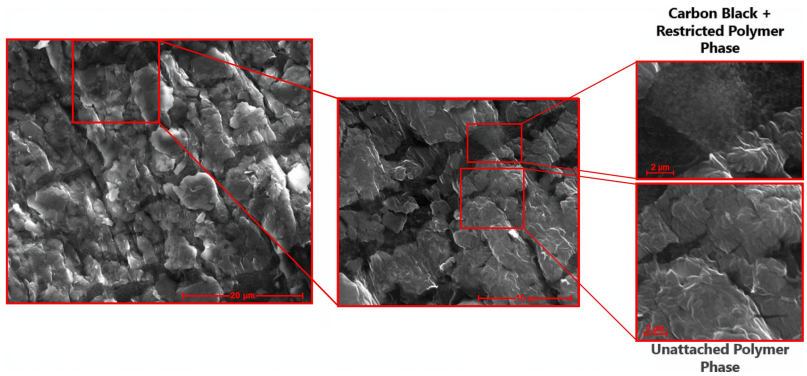

introduced under an inert atmosphere, the formation of oily smearing wear was again observed. These findings suggest that the critical factor in smearing wear formation is not oxygen *per se*, but the presence of a radical-trapping agent.

The stability of polymeric radicals is closely correlated to the rate of metal wear of the knife abrader. A highly reactive radical is thought to primarily react internally and thus cause little wear to the scraper, whereas more stable polymer radicals attack the metal more. For example, radicals formed by NR and SBR are particularly stable in nitrogen, but readily react with oxygen in air to produce smearing wear. EPR, on the other hand, undergoes degradation to a liquid-like state by wear in air and in nitrogen, because in either case, the free radicals formed by molecular rupture undergo hydrogen-abstraction and disproportionation reactions, causing further decomposition of the polymer (Baldwin and Strate, 1972; Gent and Pulford, 1979). BR is highly reactive and therefore prefers to react internally with other polymer molecules, which can even increase crosslinking within the polymeric matrix, creating only dry debris. Finally, butyl rubber [Poly(isobutylene-co-isoprene)] is the only tested material that experiences roughly three times more wear in air than in nitrogen. This is explained by the relatively stable macro-radicals formed by the polymer itself, but the even more stable peroxy radicals which are formed with oxygen (Gent and Pulford, 1979).

Another way to influence whether and to what extent smearing wear occurs is by feeding dust into the contact zone (Schallamach, 1968a, 1968b). This was tested on an Akron Abrasion Tester, where a smaller rubber sample wheel rubbed against an abrasive wheel. The dust was either a powder mixture of silicon carbide and Fuller's earth or magnesium oxide. The results are shown in Table 2. It was demonstrated that for SBR when using magnesia, the wear under an air atmosphere is 4 to 5 times higher than under a nitrogen atmosphere. In contrast, when the powder mixture is used, the wear is slightly higher under a nitrogen atmosphere. The given reasons are that magnesium oxide has shown lubrication properties (Grosch K A, 1963) and is an effective adsorber of smearing wear. Fuller's Earth, on the other hand, is a poor adsorber and has a particle size some 70 times larger than magnesia, which makes it a better abrasive. However, the performance of magnesia as a solid lubricant has only been evaluated in air (Scharf and Prasad, 2013), and its lubricating properties may not be transferable to other environments. Nevertheless, the presence of magnesia as a lubricating agent could account for the observed reduction in abrasion rates. An open question remains: If magnesia inhibits the friction-reducing effect of smearing, why is the abrasion rate in air still higher than in nitrogen? One possible explanation is that, in air, the smeared wear material is continuously formed but

Table 2 Abrasion rates of styrene-butadiene rubber (SBR) and natural rubber (NR) with nonox HFN (90 % phenyl-p-naphthylamine, 10 % diphenyl p-phenylenediamine) added as an antioxidant (AO), NR without AO, and ethylene-propylene rubber (EPR) without AO, under different atmospheres, abrasion wheels and dust, adapted from Schallamach (1968a, 1968b)

		Abrasion rate in mm^3/500 rev.			
Counterbody	**Atmosphere**	**SBR (AO)**	**NR (AO)**	**NR (-)**	**EPR (-)**
Grinding wheel, powder mixture	Air	25.2	42.5	66.5	43.1
	Nitrogen	27.0	30.6	36.4	29.4
Aluminium wheel, powder mixture	Air	9.6	8.0	12.2	-
	Nitrogen	13.2	14.8	15.8	-
Aluminium wheel, magnesia	Air	10.7	25.4	40.2	-
	Nitrogen	2.0	5.2	5.9	-
Steel wheel, powder mixture	Air	14.8	30.8	48.5	-
	Nitrogen	20.9	23.0	26.8	-
Steel wheel, magnesia	Air	25.4	52.7	75.0	-
	Nitrogen	7.8	11.9	12.2	-

immediately re-adsorbed, preventing the development of a stable, protective tribolayer.

It is now evident that oxygen plays a crucial role in the formation of smearing wear. Consequently, the presence of antioxidants (AOs) in the rubber compound may also significantly influence this process. Indeed, as shown in Table 2, natural rubber compounds without AOs exhibit abrasion rates approximately 50% higher in air compared to those containing AOs, a trend that is consistently observed across all experimental conditions.

A different study using a blade abrader in air (Pulford, 1983) investigated three CB-reinforced NR compounds, two of which contained different AOs. Under low frictional force, the NR compound without AO exhibited approximately three times higher wear compared to those with AOs. As the applied force increased, the nature of the wear debris changed: at a certain threshold, it transitioned to a powdery form, suggesting the onset of a different, more abrasive wear mechanism.

Another noteworthy observation from Table 2 is that, for SBR, the influence of the surrounding atmosphere on abrasion behavior appears to be less pronounced when tested against a rough surface (grinding wheel), which is also supported by other findings (Uchiyama, 1986).

Measuring the impact of ozone was done by comparing the abrasion of EPR, which is quite resistant to ozone, to NR with an AO. No noticeable difference in abrasion can be seen in Table 2. Also, fragmentary experiments were carried out in air that passed through a saturated potassium iodine solution to break down any ozone, and again, no change in the abrasion rates was measured. This could indicate that oxygen, rather than ozone, is the driving factor in the formation of smearing wear.

The effect of humidity on the abrasion rates was also investigated (Schallamach, 1968a, 1968b). In general, wear increased more for NR with no AO than for NR with AO or SBR, and even decreased for polybutadiene rubber (BR). The measured difference increased with rising humidity. Part of the effect could also be due to the trivial fact that more dust sticks to the sample in a humid atmosphere, but this would not explain the result of the BR compound.

The effect of debris accumulation in the wear zone was investigated by (M Huang *et al.*, 2018) using a tribometer. Their results showed that longer wear cycles led to greater accumulation of debris on the wear track, which in turn corresponded to a reduction in the overall wear rate. The study concluded that smearing wear generally exerts a *protective effect* against further abrasive wear by forming a layer that partially shields the underlying rubber surface.

Chemical degradation of tire tread can also lead to the formation of nanoparticles through volatilization processes. In a study by (Park *et al.*, 2017), tire samples were heated in a reaction chamber, with a controlled airflow directing the emitted particles to a measurement system. A significant increase in particle generation was observed once the tread temperature exceeded 160°C, with particle concentration rising exponentially up to 350°C. The resulting particle size distribution was unimodal and followed a log-normal profile, centered between 60 nm to 100 nm. While higher temperatures increased the number of particles without altering the size distribution, slower cooling rates produced larger particles. Unlike the elongated, sausage-like morphology commonly observed in road wear particles(Adachi and Tainosho, 2004; Kreider *et al.*, 2010), the particles formed in this study were nearly spherical and composed primarily of carbon, oxygen, silicon, and sulfur – elements derived from the rubber compound. These findings support a formation mechanism involving the volatilization of organic compounds in the tire tread due to frictional heating, followed by gas-phase condensation into nanoparticles.

5. Conclusion

This work provides an overview of the three primary tire wear mechanisms, outlining the conditions under which they occur and their relationship to the formation of wear particles, see Table 3.

Abrasion on a rough surface and under high normal pressure results in a high tearing energy. Under these conditions, cut-and-chip wear occurs, where particles are ripped from the bulk rubber material. It was found that, at least for an HNBR disk abraded by quartz, the particle size is proportional to the tearing energy.

On smoother surfaces, where tearing energy is lower, fatigue wear becomes the dominant mechanism. The stick-slip motion of rubber against the surface creates a stress field that promotes crack propagation, forming characteristic wear patterns. It is assumed that the size of the resulting particles is related to the spacing of these patterns, which is influenced by factors such as applied load, coefficient of friction, Young's modulus, the counterbody surface, temperature, and possibly other yet unidentified parameters.

At low normal loads, tearing energy is minimal and chemical wear dominates. In this regime, a sticky, oily film forms on the rubber surface, composed of oxidized and de-crosslinked polymer chains. This layer can act as a lubricant, generally reducing wear rates. However, at temperatures above 160°C, nanoparticles may form through volatilization processes.

It is worth noting that much of the foundational research into tire wear was conducted over 30–70 years ago. These studies often used experimental setups that are now considered

Table 3 Overview of the attributes associated with each wear mechanism, the approaches used to predict particle size, and the inherent limitations and uncertainties of such predictions

Mechanism	Condition	Particle size	Particle shape	Particle size predictability	Limitations
Cut and chip wear	High tearing energy	100 μm to 10 mm	elongated	Proportional to tearing energy	Only one experiment on HNBR
Fatigue wear	Medium tearing energy	1 μm to 100 μm	elongated	Proportional to pattern spacing	Only hypothetical, no direct evidence
Chemical wear	Low tearing energy	/	liquid	/	/
Volatilization	High temperature	1 nm to 1 μm	spherical	Inverse proportional to cooling rate	Temperature distribution in tires is complex

outdated. Moreover, different experimental methods, parameters, and protocols make direct comparison of results difficult, which consequently can lead to results that seem inconclusive or even contradictory.

With advances in materials science, imaging techniques, and computational modeling, there is a significant opportunity to revisit tire wear phenomena using modern methods. These developments open the way for future studies that combine tribological testing with particle characterization, thereby enabling a deeper understanding of tire wear processes and the underlying mechanisms. Emerging research efforts already illustrate this potential, for example: standardizing tire wear particle emission studies (Mennekes and Nowack, 2022); using finite element simulation software, with data from sensors embedded in tires, to feed a neural network-based tire wear algorithm (Li *et al.*, 2021); focusing on environmental damage in other domains such as soil (Ding *et al.*, 2023); or evaluating the toxicity of certain tire compounds, e.g. the antioxidant 6PPD (Chen *et al.*, 2023).

A deeper understanding of the interplay between tire wear mechanisms will not only enhance tire durability but also inform strategies for reducing the environmental impact of tire-derived particles.

References

Aatmeeyata, Kaul, D.S. and Sharma, M. (2009), "Traffic generated non-exhaust particulate emissions from concrete pavement: a mass and particle size study for two-wheelers and small cars", *Atmospheric Environment*, Vol. 43 No. 35, pp. 5691-5697.

Adachi, K. and Tainosho, Y. (2004), "Characterization of heavy metal particles embedded in tire dust", *Environment International*, Vol. 30 No. 8, pp. 1009-1017.

Aghababaei, R., Warner, D.H. and Molinari, J.F. (2016), "Critical length scale controls adhesive wear mechanisms", *Nature Communications*, Vol. 7 No. 1.

Allen, J.O., Alexandrova, P.E.O. and Kaloush, K.E. (2006), Tire Wear Emissions for Asphalt Rubber and Portland Cement Concrete Pavement Surfaces Arizona Department of Transportation Contract KR-04-0720-TRN Final Report. Technical report.

Anderson, J.O., Thundiyil, J.G. and Stolbach, A. (2012), "Clearing the air: a review of the effects of particulate matter air pollution on human health".

Baldwin, F.P. and Strate, G.V. (1972), "Polyolefin elastomers based on ethylene and propylene", volume 3. 45 edition.

Beatty, J.R. and Miksch, B.J. (1982), "A laboratory cutting and chipping tester for evaluating off-the-road and heavy-duty tire treads", American Chemical Society, Philadelphia.

Bergmann, M., Kirchner, U., Vogt, R. and Benter, T. (2009), "On-road and laboratory investigation of low-level PM emissions of a modern diesel particulate filter equipped diesel passenger car", *Atmospheric Environment*, Vol. 43 No. 11, pp. 1908-1916.

Boucher, J. and Friot, D. (2017), Primary Microplastics} in the Oceans: A Global Evaluation of Sources. Technical report, IUCN, Gland, Switzerland.

Bowden, F.P. and Tabor, D. (2001), *The Friction and Lubrication of Solids*, volume 1. Oxford University Press Inc., New York.

Brink, T. and Molinari, J.F. (2019), "Adhesive wear mechanisms in the presence of weak interfaces: insights from an amorphous model system", *Physical Review Materials*, Vol. 3 No. 5.

Browne, M.A., Galloway, T. and Thompson, R. (2007), Microplastic—An Emerging Contaminant} of Potential Concern? Technical report.

Cadle, S.H. and Wiliiams, R.L. (1978), "Gas and particle emissions from automobile tires in laboratory and field studies", *Journal of the Air Pollution Control Association*, Vol. 28 No. 5, pp. 502-507.

Chae, Y. and An, Y.J. (2017), "Effects of micro- and nanoplastics on aquatic ecosystems: current research trends and perspectives", *Marine Pollution Bulletin*, Vol. 124 No. 2, pp. 624-632.

Chen, X., He, T., Yang, X., Gan, Y., Qing, X., Wang, J. and Huang, Y. (2023), "Analysis, environmental occurrence, fate and potential toxicity of tire wear compounds 6PPD and 6PPD-quinone".

Cinaralp, F. (2015), End-of-life tyre report. Technical report, EUROPEAN TYRE & RUBBER manufacturer's association.

Dannis, M.L. (1974), "Rubber dust from the normal wear of tires", *Rubber Chemistry and Technology*, Vol. 47 No. 4, pp. 1011-1037.

Ding, J., Lv, M., Zhu, D., Leifheit, E.F., Chen, Q.L., Wang, Y. Q., Chen, L.X., Rillig, M.C. and Zhu, Y.G. (2023), "Tire wear particles: an emerging threat to soil health".

Essel, R., Engel, L., Carus, M. and Ahrens, R.H. (2015), "Sources of microplastics relevant to marine protection in Germany", *Texte*, Vol. 64 No. 2015, pp. 1219-1226.

European Commission (2024), "Regulation (EU) 2024/1257 of the european parliament and of the council of 24 april 2024 on type-approval and market surveillance of motor vehicles and engines (euro 7)", *Journal of the European Union*, (L 125/1).

Evstratov, V. (1967), "The mechanism of wear of tread rubbers. Abrasion of rubber".

Fortunato, G., Ciaravola, V., Furno, A., Scaraggi, M., Lorenz, B. and Persson, B.N. (2017), "Dependency of rubber friction on normal force or load: theory and experiment", *Tire Science and Technology*, Vol. 45 No. 1, pp. 25-54.

Fukahori, Y. and Yamazaki, H. (1994a), "Mechanism of rubber abrasion part 2. General rule in abrasion pattern formation in rubber-like materials", *Technical Report*.

Fukahori, Y. and Yamazaki, H. (1994b), "Mechanism of rubber abrasion. Part I: abrasion pattern formation in natural rubber vulcanizate", *Wear*, Vol. 171 Nos 1-2, pp. 195-202.

Fukahori, Y. and Yamazaki, H. (1995), "Mechanism of rubber abrasion part 3: how is friction linked to fracture in rubber abrasion? ", *Technical Report*.

Fukahori, Y., Gabriel, P., Liang, H. and Busfield, J.J. (2020), "A new generalized philosophy and theory for rubber friction and wear", *Wear*, pp. 446-447.

Gao, C., Kuhlman-Wilsdorf, D. and Makel, D.D. (1994), "The dynamic analysis of stick-slip motion", *Wear*, Vol. 173 Nos 1-2, pp. 1-12.

Garg, B.D., Cadle, S.H., Mulawa, P.A., Groblicki, P.J., Laroo, C. and Parr, G.A. (2000), "Brake wear particulate matter emissions", *Environmental Science & Technology*, Vol. 34 No. 21, pp. 4463-4469.

Gent, A.N. and Pulford, C.T. (1983), "Mechanisms of rubber abrasion", *Journal of Applied Polymer Science*, Vol. 28 No. 3, pp. 943-960.

Gent, A.N. and Pulford, C.T.R. (1979), "Wear of metal by rubber", *Technical Report*,

Grigoratos, T. and Martini, G. (2014), *Non-Exhaust Traffic Related emissions*, Brake and Tyre Wear PM, *Report EUR, 26648*, Publications Office of the European Union, Luxembourg.

Grosch, K.A. (1963), "The relation between the friction and visco-elastic properties of rubber", *Proceedings of the Royal Society of London. Series A. Mathematical and Physical Sciences*, Vol. 274 No. 1356, pp. 21-39.

Grosch, K.A. and Schallamach, A. (1961), "Tire wear at controlled slip", *Wear*, Vol. 4 No. 5, pp. 356-371.

Gustafsson, M., Blomqvist, G., Gudmundsson, A., Dahl, A., Jonsson, P. and Swietlicki, E. (2009), "Factors influencing PM10 emissions from road pavement wear", *Atmospheric Environment*, Vol. 43 No. 31, pp. 4699-4702.

Huang, M., Guibert, M., Thévenet, J., Loubet, J.L. and Sotta, P. (2018), "A new test method to simulate low-severity wear conditions experienced by rubber tire materials".

Hussein, T., Johansson, C., Karlsson, H. and Hansson, H. C. (2008), "Factors affecting non-tailpipe aerosol particle emissions from paved roads: on-road measurements in Stockholm, Sweden", *Atmospheric Environment*, Vol. 42 No. 4, pp. 688-702.

Ivel, J., Watson, R., Abbassi, B. and Abu-Hamatteh, Z.S. (2020), " Life cycle analysis of concrete and asphalt used in road pavements", *Environmental Engineering Research*, Vol. 25 No. 1, pp. 52-61.

Kole, P.J., Löhr, A.J., Van Belleghem, F.G. and Ragas, A.M. (2017), "Wear and tear of tyres: a stealthy source of microplastics in the environment",

Koliolios, E., Nakano, S., Kawamura, T. and Busfield, J.J. (2024), "Elucidation of smear wear layer structure and ageing mechanisms of filled tyre tread compounds", *Polymer*, Vol. 300.

Kreider, M.L., Panko, J.M., McAtee, B.L., Sweet, L.I. and Finley, B.L. (2010), "Physical and chemical characterization of tire-related particles: comparison of particles generated using different methodologies", *Science of The Total Environment*, Vol. 408 No. 3, pp. 652-659.

Kupiainen, K.J., Tervahattu, H., Räisänen, M., Mäkelä, T., Aurela, M. and Hillamo, R. (2005), "Size and composition of airborne particles from pavement wear, tires, and traction sanding", *Environmental Science & Technology*, Vol. 39 No. 3, pp. 699-706.

Lassen, C., Hanse, S.F., Magnusson, K., Hartmann, N.B., Rehne Jensen, P., Nielsen, T.G. and Brinch, A. (2015), "Microplastics occurrence, effects and sources of releases to the environment in Denmark", volume 24.

Li, B., Quan, Z., Bei, S., Zhang, L. and M., H., (2021), "An estimation algorithm for tire wear using intelligent tire concept", *Proceedings of the Institution of Mechanical Engineers, Part D: Journal of Automobile Engineering*, Vol. 235 Nos 10-11, pp. 2712-2725.

Lundberg, J., Gustafsson, M., Janhäll, S., Eriksson, O., Blomqvist, G. and Erlingsson, S. (2020), "Temporal variation of road dust load and its size distribution—a comparative study of a porous and a dense pavement", *Water, Air, & Soil Pollution*, Vol. 231 No. 12.

McCarty, K., Mian, H.R., Chhipi-Shrestha, G., Hewage, K. and Sadiq, R. (2023), "Ecological risk assessment of tire and road wear particles: a preliminary screening for freshwater sources in Canada", *Environmental Pollution*, Vol. 325.

Mennekes, D. and Nowack, B. (2022), "Tire wear particle emissions: measurement data where are you? ", *Science of The Total Environment*, Vol. 830.

Mueller, B.C., Brumbelow, M.L., Bragg, H. and Jermakian, J. S. (2024), "Comparison of frontal crash compatibility metrics between battery-electric and internal-combustion-engine passenger vehicles", *Traffic Injury Prevention*, Vol. 25 No. 5, pp. 750-756.

Muhr, A.H. and Roberts, A.D. (1992), "Rubber abrasion and wear", *Technical Report*.

Muhr, A., Pond, T. and Thomas, A. (1987), "Abrasion of rubber and the effect of lubricants", *Journal de Chimie Physique*, Vol. 84, pp. 331-334.

Muratori, M., Alexander, M., Arent, D., Bazilian, M., Dede, E.M., Farrell, J., Gearhart, C., Greene, D., Jenn, A., Keyser, M., Lipman, T., Narumanchi, S., Pesaran, A., Sioshansi, R., Suomalainen, E., Tal, G., Walkowicz, K. and Ward, J. (2021), "The rise of electric vehicles-2020 status and future expectations".

Nakano, S., Yamahashi, Y., Kaneko, F., Zushi, T., Mabuchi, T., Kawamura, T. and Tada, T. (2021), "Effect of molecular structure on the mechanochemical wear behavior of hydrogenated and conventional sbr rubbers", *KGK Kautschuk Gummi Kunststoffe*, Vol. 74 No. 1, pp. 56-61.

Nguyen, V.H., Zheng, D., Schmerwitz, F. and Wriggers, P. (2017), "An advanced abrasion model for tire wear".

Panko, J., Mcatee, B.L., Kreider, M., Gustafsson, M., Blomqvist, G., Gudmundsson, A., Sweet, L. and Finley, B. (2009), "Physio-chemical analysis of airborne tire wear particles", ChemRisk.

Park, I., Lee, J. and Lee, S. (2017), "Laboratory study of the generation of nanoparticles from tire tread", *Aerosol Science and Technology*, Vol. 51 No. 2, pp. 188-197.

Persson, B.N. and Volokitin, A.I. (2006), "Rubber friction on smooth surfaces", *The European Physical Journal E*, Vol. 21 No. 1, pp. 69-80.

Piscitello, A., Bianco, C., Casasso, A. and Sethi, R. (2021), "Non-exhaust traffic emissions: sources, characterization, and mitigation measures".

Pulford, C.T. (1983), "Antioxidant effects during blade abrasion of natural rubber", *Journal of Applied Polymer Science*, Vol. 28 No. 2, pp. 709-713.

Saibel, E. and Tsai, C. (1969), "Tire wear model",

Schallamach, A. (1954), "On the abrasion of rubber", *Technical Report*.

Schallamach, A. (1955), "Zur physik der kautschukreibung", *Kolloid-Zeitschrift*, Vol. 141 No. 3, pp. 165-173.

Schallamach, A. (1957), "Frictional temperature rises on rubber", *Rubber Chemistry and Technology*, Vol. 30 No. 4, pp. 1097-1102.

Schallamach, A. (1958), "Friction and abrasion of rubber", *Wear*, Vol. 1 No. 5, pp. 384-417.

Schallamach, A. (1963), "A theory of dynamic rubber friction", *Wear*, Vol. 6 No. 5, pp. 375-382.

Schallamach, A. (1968a), "Recent advances in knowledge of rubber friction and tire wear", *Rubber Chemistry and Technology*, Vol. 41 No. 1, pp. 209-244.
Schallamach, A. (1968b), "Abrasion, fatigue, and smearing of rubber", *Journal of Applied Polymer Science*, Vol. 12 No. 2, pp. 281-293.
Scharf, T.W. and Prasad, S.V. (2013), "Solid lubricants: a review".
Setiyana, B., Khafidh, M., Tauviqirrahman, M., Ismail, R., Jamari. and Schipper, D.J. (2021), "Friction and wear pattern of silica-reinforced styrene-butadiene rubber (SBR) in sliding contact with a blade indenter", *Lubricants*, Vol. 9 No. 11.
Simons, A. (2016), "Road transport: new life cycle inventories for fossil-fuelled passenger cars and non-exhaust emissions in ecoinvent v3", *The International Journal of Life Cycle Assessment*, Vol. 21 No. 9, pp. 1299-1313.
Sjödin, Ferm, M., Björk, A., Rahmberg, M., Gudmundsson, A. and Swietlicki, E. (2010), Wear particles from road traffic-a field, laboratory and modelling study Final report. Technical report, IVL Swedish Environmental Research Institute Ltd.
Sommer, F., Dietze, V., Baum, A., Sauer, J., Gilge, S., Maschowski, C. and Gieré, R. (2018), "Tire abrasion as a major source of microplastics in the environment", *Aerosol and Air Quality Research*, Vol. 18 No. 8, pp. 2014-2028.
Southern, E. and Thomas, A.G. (1978), "Studies of rubber abrasion".
Stoček, R., Mars, W.V., Kipscholl, R. and Robertson, C.G. (2019), "Characterisation of cut and chip behaviour for NR, SBR and BR compounds with an instrumented laboratory device", *Plastics, Rubber and Composites*, Vol. 48 No. 1, pp. 14-23.
Stoček, R., Heinrich, G., Kipscholl, R. and Kratina, O. (2021a), "Cut & chip wear of rubbers in a range from low up to high severity conditions", *Applied Surface Science Advances*, Vol. 6.
Stoček, R., Ghosh, P., Machů, A., Chanda, J. and Mukhopadhyay, R. (2021b), "Fatigue crack growth vs. Chip and cut wear of NR and NR/SBR Blend-Based rubber compounds", *Advances in Polymer Science*, Springer Nature Switzerland, Vol. 286, pp. 225-244.
Suh, N.P. (1973), "The delamination theory of wear", *Technical Report*.
Sundt, P., Schulze, P.-E. and Syversen, F. (2014), "Sources of microplastic-pollution to the marine environment", *Mepex for the Norwegian Environment Agency*, Vol. 86, p. 20.
Thavamani, P. and Bhowmick, A.K. (1992), "Wear of tank track pad rubber vulcanizates by various rocks", *Rubber Chemistry and Technology*, Vol. 65 No. 1, pp. 31-45.
Thavamani, P. and Bhowmick, A.K. (1993), Influence of compositional variables and testing temperature on the wear of hydrogenated nitrile rubber. Technical Report 11993.
Timmers, V.R. and Achten, P.A. (2016), "Non-exhaust PM emissions from electric vehicles".
Treloar, L.G. (1975), "The physics of rubber elasticity".
Truong, X.T., Muresan, B., Lumiere, L., Liu, Y. and Cerezo, V. (2025), "Morphological and textural characteristics of tire-road wear particles linked to different wear mechanisms", *Wear*, Vol. 571.
Uchiyama, Y. (1986), "The effect of environment on the friction and wear of rubber", *Wear*, Vol. 110 Nos 3-4, pp. 369-378.
Uchiyama, Y. and Ishino, Y. (1992), "Pattern abrasion mechanism of rubber", *Technical Report*.
Wagner, S., Hüffer, T., Klöckner, P., Wehrhahn, M., Hofmann, T. and Reemtsma, T. (2018), "Tire wear particles in the aquatic environment – A review on generation, analysis, occurrence, fate and effects".
Wagner, M., Scherer, C., Alvarez-Muñoz, D., Brennholt, N., Bourrain, X., Buchinger, S., Fries, E., Grosbois, C., Klasmeier, J., Marti, T., Rodriguez-Mozaz, S., Urbatzka, R., Vethaak, A.D., Winther-Nielsen, M. and Reifferscheid, G. (2014), "Microplastics in freshwater ecosystems: what we know and what we need to know", *Environmental Sciences Europe*, Vol. 26 No. 1, pp. 1-9.
Weiss, M., Irrgang, L., Kiefer, A.T., Roth, J.R. and Helmers, E. (2020), "Mass- and power-related efficiency trade-offs and CO2 emissions of compact passenger cars", *Journal of Cleaner Production*, Vol. 243.
Wik, A. and Dave, G. (2009), "Occurrence and effects of tire wear particles in the environment - A critical review and an initial risk assessment".
Wu, A. and Shi, X. (2013), "Numerical investigation of adhesive wear and static friction based on the ductile fracture of junction", *Journal of Applied Mechanics*, Vol. 80 No. 4.
Wu, G., Sotta, P., Huang, M., Tunnicliffe, L.B. and Busfield, J.J.C. (2023), "Characterization of sticky debris generated during smear wear", *Rubber Chemistry and Technology*, Vol. 96 No. 4, pp. 588-607.
Xu, R., Sheng, W., Zhou, F. and Persson, B.N. (2025), "Rubber wear: history, mechanisms, and perspectives".
Yadav, J.S. and Tiwari, S.K. (2017), "The impact of end-of-life tires on the mechanical properties of fine-grained soil: a review".
Zhang, H., Goltsberg, R. and Etsion, I. (2022), "Modeling adhesive wear in asperity and rough surface contacts: a review".
Zhang, M., Yin, H., Tan, J., Wang, X., Yang, Z., Hao, L., Du, T., Niu, Z. and Ge, Y. (2023), "A comprehensive review of tyre wear particles: formation, measurements, properties, and influencing factors", *Atmospheric Environment*, Vol. 297, p. 119597.

Corresponding author

Alexander Schmiedhofer can be contacted at: alexander.schmiedhofer@tuwien.ac.at